

Conductance anomalies in a one-dimensional quantum contact

O.P. Sushkov

*School of Physics, University of New South Wales,
Sydney 2052, Australia*

Short length quantum wires (quantum contacts) exhibit a conductance structure at the value of conductance close to $0.7 \times 2e^2/h$. The structure is also called the conductance anomaly. In longer contacts the structure evolves to the lower values of conductance. We demonstrate that this structure is related to the development of charge density waves within the contact. This is a precursor for Wigner crystallization. Many-body Hartree-Fock calculations of conductance are performed. The results are in agreement with experimental data.

PACS: 73.61.-r, 73.23.Ad, 71.45.Lr

I. INTRODUCTION

The quantized conductance $G = nG_2$, $n = 1, 2, 3, \dots$, $G_2 = 2e^2/h$, through a narrow quantum point contact was discovered in 1988^{1,2}. This quantization can be understood within a one-dimensional (1D) non-interacting electron gas picture, see e.g. Ref.³. In the present work we are interested in a deviation from the integer quantization. This deviation, the so called “0.7 anomaly” has been found in experimental works^{4,5}. The anomaly is a shoulder-like feature or a narrow plateau at $G \approx 0.7G_2$. The recent work⁶ demonstrates that the anomaly evolves down to $G \approx 0.5G_2$ in longer quantum contacts. Another highly interesting recent experimental development is an indication of the above barrier excitation⁷. The excitation is probably related to the “0.7 anomaly”.

There is practically no doubt that the structure is due to the interaction between the electrons. There have been numerous attempts to explain the “0.7 anomaly” by spontaneous magnetization of the 1D quantum wire due to exchange Coulomb interaction^{8–11}. A somewhat similar, but still different idea is to explain the anomaly by formation of a two-electron bound state with total spin $S = 1$, see Refs.^{12,13}.

It is not clear why the spontaneous magnetization scenario can be valid since it contradicts to the rigorous Lieb-Mattis theorem¹⁴. The theorem claims that any 1D many-body system with quadratic kinetic energy and with a potential interaction has the ground state with zero spin. The same argument is applicable to the $S=1$ bound state picture. Strictly speaking in the later case one can avoid a formal contradiction with the theorem saying that the bound state is localized somewhere in the transition region between the 2D or 3D conductor and the 1D wire. However this scenario seems unlikely and in the present work I consider only $S=0$ ground state in accordance with Lieb-Mattis theorem.

The effect of Wigner crystallization in low density 2D and 3D electron gas is well known. There is no such a thing as an ideal 1D Wigner crystal because quantum fluctuations destroy any long range order. However it was pointed out some time ago¹⁵ that impurities suppress the fluctuations and pin the 1D Wigner crystal. Surprisingly this happens at pretty high density of electrons n : $n \approx 0.5/a_B$, where a_B is the Bohr radius. A quantum contact (=short quantum wire) is not uniform and hence it pins the crystal. This must result in nontrivial behavior of the contact conductance. It is the effect we study in the present work using the Hartree-Fock (HF) method. We demonstrate that the effect results in the conductance anomaly at $G \approx 0.7G_2$ for a short contact and in several anomalies for longer contacts. In the present work we consider only zero temperature case. However in conclusions we comment on temperature dependence.

The idea of relation between the conductance anomaly and the Wigner crystallization was also suggested in a recent paper¹⁶. Authors of this paper discuss a ferromagnetic state embedded in the Wigner crystal. We follow the different way considering the ground state with total spin zero in accordance with Lieb-Mattis theorem.

In independent particle approximation, i.e. in the case of an ideal electron gas, a calculation of the conductance for a given transverse channel is straightforward. Assuming adiabatic transmission one gets

$$G = \frac{2e^2}{h}T, \quad (1)$$

where T is the barrier transmission probability at Fermi energy^{17,3}. In the case of interacting particles this formula is also valid because before and after the potential barrier the density of electrons is high enough,

and hence the interaction is negligible. However one can not use the single particle description to calculate the transmission probability T because in the vicinity of the barrier the electron density is low, and hence the many-body effects are very important. The main question is how to calculate the transmission probability T ? To do this we apply the following trick. Consider the liquid of electrons on a 1D ring with a potential barrier somewhere on the ring. There is no current in the ground state of the system. Now let us apply a magnetic flux through the ring. This flux induces the electric current. On the one hand the current is related to the barrier transmission probability T . On the other hand, the current can be calculated using the HF method. This allows us to find T with account of many-body effects.

Structure of the present paper is the following: The relation between the current on the ring and the transmission probability is derived in Sec. II. In Sec. III we demonstrate how the Hartree-Fock method describes development of the charge-density wave at low electron density. The results of selfconsistent calculations of the transmission probabilities for different barriers are presented in Sec. IV. Sec. V summarizes the results and presents our conclusions.

II. RELATION BETWEEN THE BARRIER TRANSMISSION PROBABILITY AND THE CURRENT IN THE RING INDUCED BY THE MAGNETIC FLUX.

Let us consider a single particle in a potential $U(x)$. The potential is localized near $x = 0$, $U(x) = 0$ at $|x| > l/2$. For simplicity we assume that the potential is symmetric, $U(x) = U(-x)$. In the scattering problem the wave function outside the region of the potential is of the form

$$\begin{aligned} x < -l/2: \quad \chi &= e^{ikx} + Ae^{-ikx}, \\ x > l/2: \quad \chi &= Be^{ikx}, \end{aligned} \quad (2)$$

where $k = \sqrt{2E}$ is the momentum of the particle, A is the reflection amplitude and B is the transmission amplitude. Throughout the paper we set the electron mass, electric charge, and the Planck constant equal to unity, $m = e = \hbar = 1$. The transmission probability is $T = |B|^2$. One can also use the basis of standing waves. Since the potential is symmetric, there is one symmetric and one antisymmetric solution at a given energy E

$$\begin{aligned} x < -l/2: \quad \chi_{\pm} &= \cos(kx + \delta_{\pm}), \\ x > l/2: \quad \chi_{\pm} &= \pm \cos(kx - \delta_{\pm}). \end{aligned} \quad (3)$$

Comparing eqs. (2) and (3) one can express the transmission and reflection amplitudes in terms of the scattering phases

$$\begin{aligned} A &= e^{-i\Delta} \cos \delta, \\ B &= -ie^{-i\Delta} \sin \delta, \\ T &= |B|^2 = \sin^2 \delta, \end{aligned} \quad (4)$$

where

$$\begin{aligned} \Delta &= \delta_+ + \delta_-, \\ \delta &= \delta_+ - \delta_-. \end{aligned} \quad (5)$$

Now we switch the vector potential \mathcal{A} on

$$H = \frac{(p - \mathcal{A})^2}{2} + U(x), \quad (6)$$

and close the ring imposing the periodic boundary condition

$$\psi(-L/2) = \psi(L/2). \quad (7)$$

We will assume that the length of the ring L is much larger than the size of the region where the potential $U(x)$ is nonzero: $L \gg l$. Note that the vector potential we introduce is the pure gauge one. We need it to induce the orbital current in the ring. The magnetic field is zero. The induced current depends only on the Bohm-Aharonov phase $\phi = \mathcal{A}L$. In the many-body problem the current has period $\Delta\phi = \pi$. The current is maximum at $\phi = \pm\pi/2, \pm3\pi/2, \dots$. For further considerations we take the first maximum

$$\mathcal{A} = \pi/2L, \quad \phi = \pi/2. \quad (8)$$

Solution of the Schrödinger equation with Hamiltonian (6),(8) and the periodic boundary condition (7) gives the following single electron wave functions outside of the region of the potential.

$$\psi_{\pm}(x) = \frac{1}{\sqrt{L(1+|a_{\pm}|^2)}} (e^{-i\Delta} e^{ikx} + a_{\pm} e^{-ikx+2iAx}) \quad (9)$$

Here $l/2 < x < L - l/2$,

$$a_{\pm} = \frac{1 \mp ie^{-i\delta}}{1 \pm ie^{-i\delta}}, \quad (10)$$

and the momentum k obeys the following quantization condition

$$e^{ikL} = \pm ie^{i\Delta}. \quad (11)$$

There are two solutions: ψ_+ and ψ_- . To elucidate meaning of these solutions let us look at two limiting cases. The first limit is an infinitely high potential barrier, $U \rightarrow \infty$. In this case the scattering phases are equal, $\delta_+ = \delta_-$. Substituting these phases into eqs. (10), (9) one finds that the wave functions ψ_{\pm} coincide with symmetric and antisymmetric standing waves (3). In the second limit there is no barrier, $U = 0$. Then the scattering phases are the following: $\delta_+ = 0$, $\delta_- = -\pi/2$. One can prove that in this case the states (9) describe clockwise and anti-clockwise rotations, $\psi_+ \rightarrow \exp(ikx)$, $\psi_- \rightarrow \exp(-ikx + 2iAx)$.

The quantization condition (11) gives the following momenta

$$k_m^{(\pm)} = \frac{2\pi}{L} (m \pm 1/4 + \Delta/2\pi), \quad m = 0, 1, 2, 3, \dots, \quad (12)$$

and energy levels

$$\begin{aligned} \epsilon_m^{(+)} &= \frac{1}{2} \left(\frac{2\pi}{L} \right)^2 (m + \Delta/2\pi)^2, \\ \epsilon_m^{(-)} &= \frac{1}{2} \left(\frac{2\pi}{L} \right)^2 (m - 1/2 + \Delta/2\pi)^2. \end{aligned} \quad (13)$$

Using the wave functions (9) one easily finds the electric current in each single particle state

$$\begin{aligned} J_m^{(+)} &= \frac{2\pi}{L^2} (m + \Delta/2\pi) \sin \delta, \\ J_m^{(-)} &= -\frac{2\pi}{L^2} (m - 1/2 + \Delta/2\pi) \sin \delta. \end{aligned} \quad (14)$$

Up to now we were considering the single particle problem. Now let us consider the many body problem. To do this we fill all the single particle states up to the Fermi energy. Each orbital state is filled by two electrons, spin up and spin down. Electric currents $J_m^{(+)}$ and $J_m^{(-)}$ partly compensate each other, so the total electric current of the many-body system is

$$\begin{aligned} J &= 2 \sum_m \left(J_m^{(+)} + J_m^{(-)} \right) = \frac{4\pi}{L^2} \sum_m \left[(m + \Delta/2\pi) (\sin \delta(k_m^{(+)}) - \sin \delta(k_m^{(-)})) + \frac{1}{2} \sin \delta(k_m^{(-)}) \right] \\ &= \frac{2\pi}{L^2} \sum_m \left[k \frac{d \sin \delta}{dk} + \sin \delta \right] = \frac{2\pi}{L^2} \sum_m \frac{d(k \sin \delta)}{dk} = \frac{1}{L} \int_0^{k_F} \frac{d(k \sin \delta)}{dk} dk = \frac{k_F}{L} \sin \delta_F = \frac{\pi N}{2L^2} \sin \delta_F. \end{aligned} \quad (15)$$

Here N is the number of electrons on the ring, $k_F = \pi N/2L$ is the Fermi momentum, and δ_F is the scattering phase δ , see eq. (5), taken at the Fermi energy.

Eq. (15) gives the main tool we use in the present work. First we solve numerically the many body problem on the ring without the barrier, $U = 0$, and find the electric current J_0 . Second we solve numerically the many body problem with the barrier, $U \neq 0$, and find the electric current J_U . Then using eqs. (15) and (4) we conclude that the transmission probability at the Fermi energy is

$$T = (J_U/J_0)^2. \quad (16)$$

This is exactly the transmission probability we need for the conductance (1).

In the derivation of eqs. (15) and (16) we neglect electron-electron interaction outside the potential barrier. This is valid if the density of electrons is high enough. In the vicinity of the barrier the electron density is low and hence the electron-electron interaction is very important. This does not contradict to the presented derivation. The information about the electron-electron interaction is hidden in the scattering phases.

Finally we would like to comment on the Luttinger liquid behavior that is related to the long-range fluctuations in the 1D interacting Fermi gas. The HF method we use to analyze the electron ring certainly does not take into account the long-range fluctuations. However this is irrelevant to the calculation of the barrier transmission probability. The matter is that the number of electrons above the quantum barrier is not more than several, so there is no room for the long-range fluctuations within the barrier. The long ring outside the barrier is just a technical trick to describe the reservoir of electrons. There is no need to take into account the long-range fluctuations in the reservoir.

III. HARTREE-FOCK (HF) METHOD FOR INTERACTING ELECTRONS ON THE RING IN THE EXTERNAL GAUGE FIELD. CHARGE-DENSITY WAVE PINNED BY THE IMPURITY.

The Hamiltonian of the many body system we consider is of the form

$$H = \sum_i \left[\frac{(p_i - \mathcal{A})^2}{2} + U(x_i) \right] + \frac{1}{2} \sum_{i,j} V(x_i, x_j), \quad (17)$$

where indexes i and j numerates electrons, x_i is the periodic coordinate ($0 < x < L$), \mathcal{A} is the gauge field (8), $U(x)$ is the potential barrier, and V_{ij} is the electron-electron interaction. We use atomic units, so coordinates are measured in unites of Bohr radius, $a_B = \epsilon \hbar^2 / m e^2$, and energies are measured in units of $E_{unit} = m e^4 / \hbar^2 \epsilon^2$, where m is the effective electron mass and ϵ is the dielectric constant. For experimental conditions of works⁴⁻⁷ these values are the following: $a_B \approx 10^{-2} \mu m$, $E_{unit} \approx 10^{-2} eV$. The electron-electron Coulomb repulsion we take in the form

$$V(x, y) = \frac{1}{\sqrt{a_t^2 + D^2(x, y)}}, \quad (18)$$

where a_t is the effective width of the transverse channel, and $D(x, y)$ is the length of the shortest arc between the points x and y on the ring, see comment¹⁸. The transverse motion of electrons is frozen due to some confining potential that can be approximated as

$$U_{\perp}(\rho) = \frac{m \omega_{\perp}^2 \rho^2}{2}. \quad (19)$$

According to the data^{7,6} the energy splitting between the transverse channels is $\hbar \omega_{\perp} \sim 4 - 7 meV$. This gives the following value of the first channel transverse size

$$a_t = 1 / \sqrt{m \omega_{\perp}} \approx 2 a_B. \quad (20)$$

Averaging over the oscillator wave function of the transverse motion shows that the effective 1D Coulomb interaction is well approximated by eq. (18). We stress that the value of a_t is close to the critical distance between the electrons at which the Wigner crystallization occurs¹⁵. This is a fortunate coincidence. Larger value of a_t would suppress the conductance anomaly, and this really happens in higher transverse channels. Substantially smaller value of a_t would require a theoretical technique more sophisticated than the HF method employed in the present work. We will discuss this point later. Let us also comment on the long-range behavior of the interaction (18). Because of the ring geometry the interaction (18) at $|x - y| \sim L$ is somewhat different from the Coulomb one. However the so long range tail of the interaction does not influence the results. Anyway in a real system there is a screening by gates and many other effects that influence the long range tail. What is important is that at the size of the barrier $|x - y| \sim l \ll L$ the interaction (18) has the right form, $V = 1/|x - y|$.

In the HF method the many body wave function of the system (17) is represented in the form of Slater determinant of single particle orbitals $\varphi_i(x)$. Each orbital obeys the equation

$$\hat{h}\varphi_i = \epsilon_i\varphi_i, \quad (21)$$

where ϵ_i is the single particle energy and \hat{h} is the HF Hamiltonian

$$\begin{aligned} \hat{h}\varphi(x) &= \left(\frac{(p - \mathcal{A})^2}{2} + U_{eff}(x) \right) \varphi(x) - \sum_j \int \varphi_j^*(y) \varphi(y) V(x, y) dy \varphi_j(x), \\ U_{eff} &= U(x) + \sum_j \int |\varphi_j(y)|^2 V(x, y) dy. \end{aligned} \quad (22)$$

Here the summation is performed over all filled orbitals. To avoid misunderstanding we have to comment on a terminological question. Usually only the case of zero vector potential, $\mathcal{A} = 0$, is called the HF method. If $\mathcal{A} \neq 0$ the method is called the Hartree-Fock method in the external field, or if \mathcal{A} is time dependent it is called the time dependent Hartree-Fock method¹⁹. The external field method is equivalent to the Random Phase Approximation (RPA). A crucial point is that the external field Hartree-Fock method (=RPA) is gauge invariant, and therefore the electric current calculated within this method is conserved²⁰.

For computations we use a ring of length $L = 80$ with a finite grid of 400 or 600 points. A naive finite grid version of the Hamiltonian (22) has a weak dependence on the gauge and hence the electric current is not exactly conserved. To avoid this minor trouble we use the lattice (=grid) modification of the Hamiltonian (22) replacing $(p - \mathcal{A})^2\varphi$ by $[2|\varphi(n)|^2 - \varphi^*(n+1)e^{iAh}\varphi(n) - \varphi^*(n)e^{-iAh}\varphi(n+1)]/2h^2$. Here h is the step of the grid and $\varphi(n)$ is the wave function on the site n of the grid. The electric current corresponding to the grid Hamiltonian is

$$J = - \sum_j \frac{i}{2h} [\varphi_j^*(n)e^{iAh}\varphi_j(n+1) - \varphi_j^*(n+1)e^{-iAh}\varphi_j(n)]. \quad (23)$$

This current is exactly conserved at a finite h , and at $h \rightarrow 0$ it coincides with the standard electric current.

First we consider the impurity pinned Wigner crystallization¹⁵. The electron density on the ring found as a result of the self consistent solution of the HF equations without any impurity, $U(x) = 0$, is plotted in Fig.1 by long dashed lines. We consider the total number of electrons $N = N_\uparrow + N_\downarrow = 78, 50, 38, 18$, $N_\uparrow = N_\downarrow$. The density is homogeneous. The density with the external potential

$$U(x) = \frac{U_0}{e^{(|x-l/2|/d) + 1}} \quad (24)$$

at $U_0 = 0.5$, $l = 8$, and $d = 1$ are shown by solid lines.

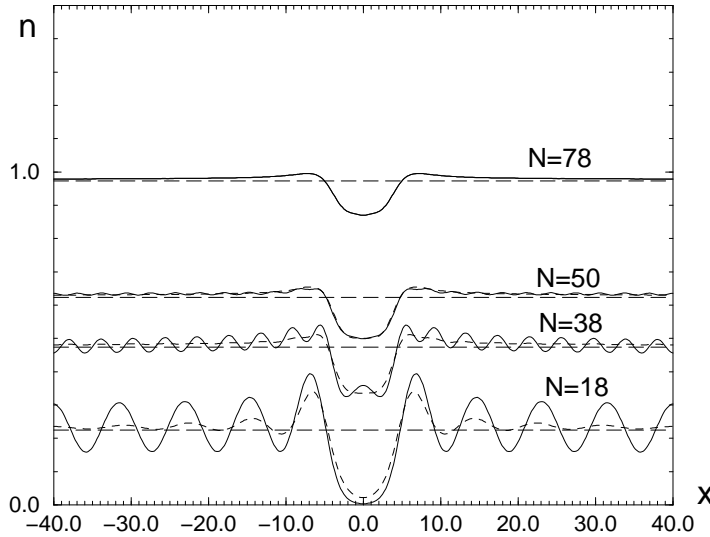


FIG. 1. The Hartree-Fock electron density on the ring without (long dashed line) and with (solid line) small impurity. The dashed line corresponds to the Hartree approximation. The number of electrons on the ring is $N = 78, 50, 38, 18$.

It is clearly seen that the impurity pinned charge density wave is developed at the electron density $n \approx 0.5$. For comparison, we also show by dashed lines the results obtained in the Hartree approximation (no exchange interaction). The Hartree approximation also gives the charge density wave but underestimates the effect. In real Wigner crystal spins are localized at the sites of the lattice. This spin structure certainly can not be obtained in the HF approximation that enforces zero spin density at any point. However we are not going to study a real Wigner crystal at very low electron density. Anyway such a state does not conduct an electric current. We are interested in $n \geq 0.5$. The charge density wave at $n \sim 0.5$ is only a precursor for the Wigner crystallization and this precursor can be described in the HF approximation.

In obtaining the results presented on Fig.1 we have used the transverse cutoff $a_t = 2$, see eqs. (18),(20). At the smaller value of a_t the charge density wave is developed at a higher electron density. This reflects the fact that the HF method with the ideal Coulomb interaction overestimates the tendency towards the charge density waves. Fortunately the value of $a_t \sim 2$ compensates this overestimation giving the correct value of the “critical” density¹⁵. This is why the application of the Hartree-Fock method is justified.

We also performed HF calculations with total spin $S \neq 0$. Technically it is very simple, we just set $N_\uparrow \neq N_\downarrow$. The macroscopic magnetization, i.e. $S \sim N$, does not arise. However, it is interesting to note that at the low electron density, $n \leq 1$, the ground state with $S = 1$ or $S = 2$ sometimes has slightly lower energy than the state with $S = 0$. This clearly contradicts to the rigorous Lieb-Mattis theorem¹⁴ and therefore it is just a byproduct of the HF approximation. We disregard this result and consider only the states with $S = 0$.

IV. MANY-BODY CALCULATION OF THE BARRIER TRANSMISSION PROBABILITY

For calculations in this section we take the number of electrons on the ring $N = N_\uparrow + N_\downarrow = 158$, $N_\uparrow = N_\downarrow$. This corresponds to the average electron density $\langle n \rangle = 1.975$ that is well above the charge density wave threshold. The external potential barrier is taken in the form (24). The parameter U_0 models the gate potential in the experiments⁴⁻⁷. Selfconsistent solution of the HF eqs. (21) is performed at $U_0 = 0$ and at $U_0 \neq 0$ and then the transmission probability is found using eq. (16). The transmission probability as a function of U_0 at $d = 0.5$ and the values of the barrier length $l = 4, 6, 8, 10, 12$ is plotted in Fig.2.

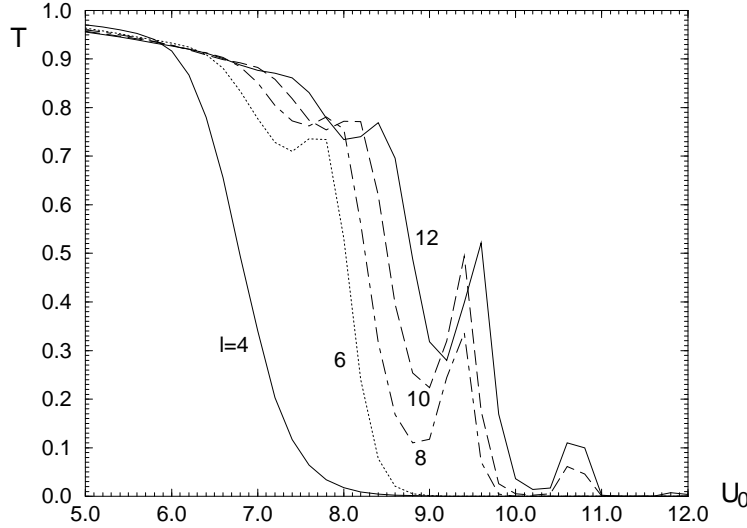


FIG. 2. The transmission probability T versus the potential U_0 . The transmission probability has been calculated in the Hartree-Fock approximation at $d = 0.5$ for the values of the barrier length $l = 4, 6, 8, 10, 12$.

The plot of T versus U_0 is representative if $L \gg l$. However in the computations $L = 80$ and therefore the inequality is not so strong. As a result the Fermi energy attains a weak U_0 dependence. To compensate this effect, in Fig.3 we plot the transmission probability T versus the value of $V_0 = U_0 - \epsilon_F(U_0) + \epsilon_F(U_0 = 0)$ that models the gate potential more accurately.

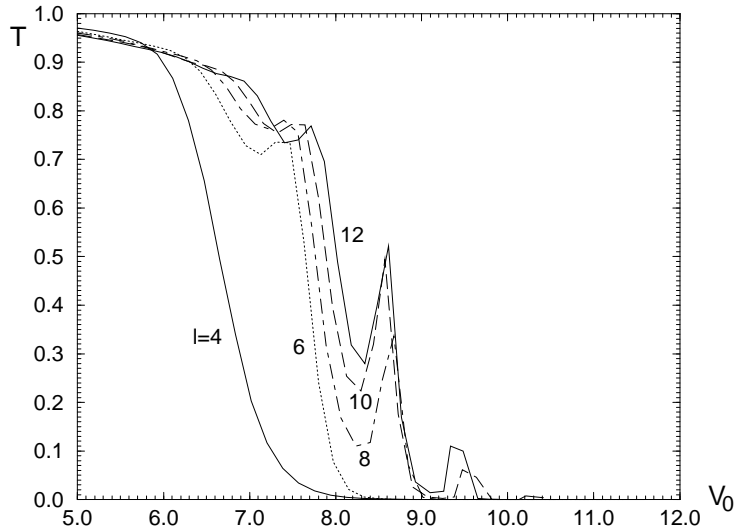


FIG. 3. The transmission probability T versus the gate potential V_0 . The transmission probability has been calculated in the Hartree-Fock approximation at $d = 0.5$ for the values of the barrier length $l = 4, 6, 8, 10, 12$.

There is no a qualitative difference between Fig.2 and Fig.3, but Fig.3 is more correct quantitatively. There are some very sharp structures in Fig.2 and Fig.3, but they arise only because of the relatively large step in U_0 . The computations are rather time consuming and this limits the number of points. For comparison we present in Fig.4 the same plots as in Fig.3, but the curves have been obtained in the Hartree approximation. So the exchange term in eq. (22) has been dropped out.

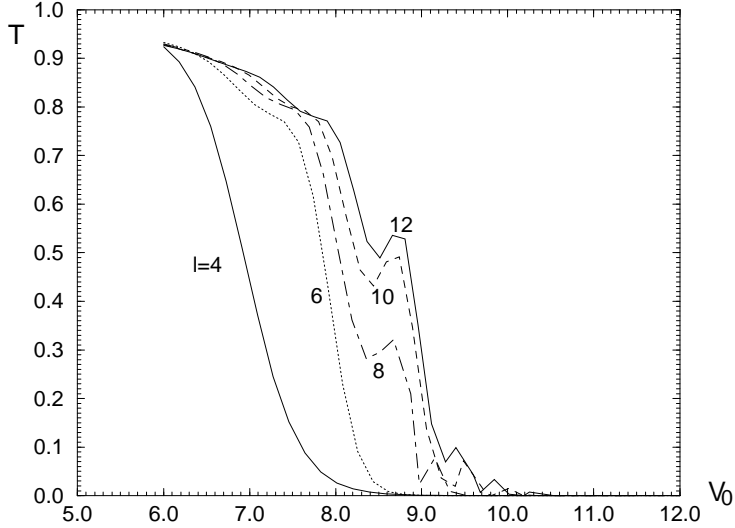


FIG. 4. The transmission probability T versus the gate potential V_0 . The transmission probability has been calculated in the Hartree approximation at $d = 0.5$ for the values of the barrier length $l = 4, 6, 8, 10, 12$.

The results of Hartree approximation are qualitatively similar to that of the HF approximation, Fig.3. However all the structures are less pronounced.

The previous figures present the barrier transmission probability calculated at the parameter $d = 0.5$, see eq. (24). In Fig.5 and Fig.6 we plot the similar results at $d = 1$. The Fig.5 corresponds to the HF approximation and Fig.6 corresponds to the Hartree approximation.

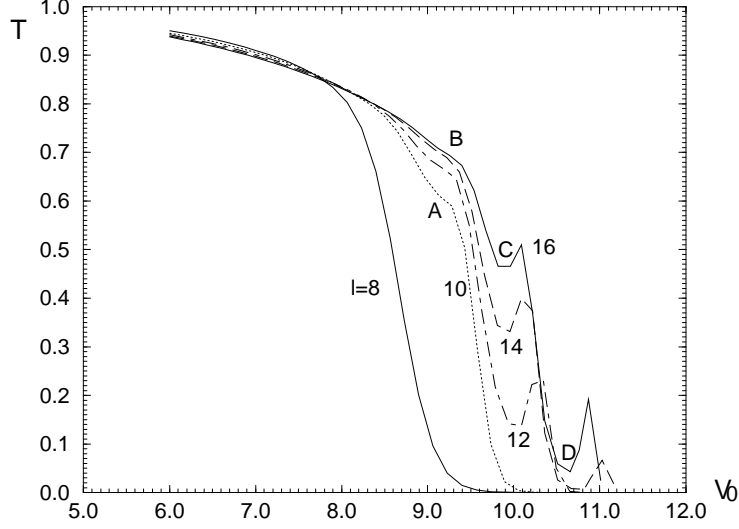


FIG. 5. The transmission probability T versus the gate potential V_0 . The transmission probability has been calculated in the Hartree-Fock approximation at $d = 1$ for the values of the barrier length $l = 8, 10, 12, 14, 16$.

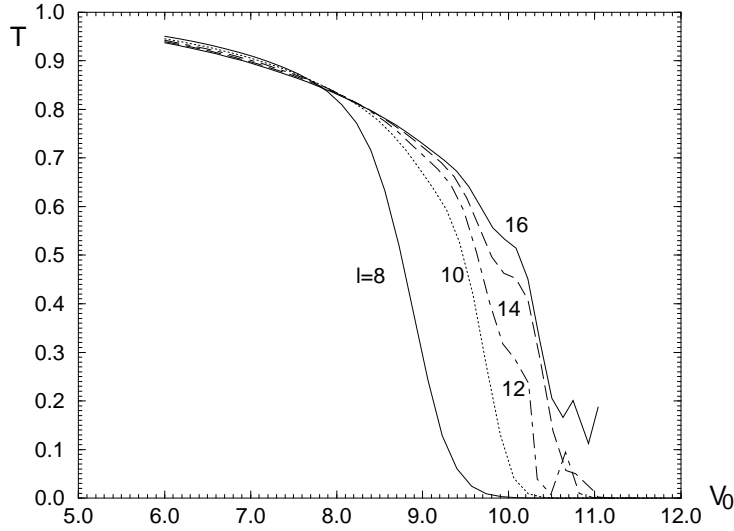


FIG. 6. The transmission probability T versus the gate potential V_0 . The transmission probability has been calculated in the Hartree approximation at $d = 1$ for the values of the barrier length $l = 8, 10, 12, 14, 16$.

The Hartree approximation gives results qualitatively similar to that of the HF approximation, but the Hartree approximation clearly underestimates the structure.

Fig.3 and Fig.5 clearly demonstrate a shoulder at the value of the transmission probability $T \sim 0.7$. For longer barriers an additional structure appears at smaller values of T . This is in agreement with experimental data⁴⁻⁷. We remind that we use the unit of length $a_B \approx 10^{-2} \mu m$, so the typical length of barriers presented in Fig.3 and Fig.5 is between $0.1 \mu m$ and $0.2 \mu m$.

To understand the reason for the structures in the transmission probability we plot the effective selfconsistent potential U_{eff} (see eq. (22)) and the electron density above the barrier at parameters corresponding to these structures. The point A in Fig.5 indicates the shoulder at $T \approx 0.65$ for the barrier of the length $l = 10$, the parameters are: $l = 10, d = 1, U_0 = 9.8$. The corresponding selfconsistent potential is shown in Fig.7 by the solid line, the external potential (24) is shown by the dashed line.

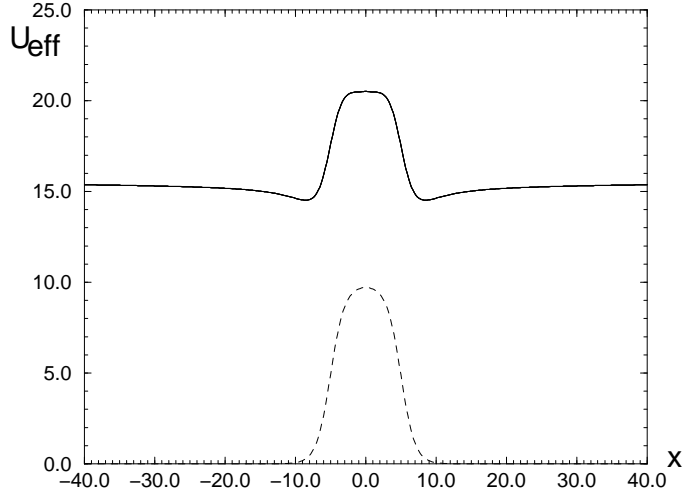


FIG. 7. The selfconsistent HF potential (22) is shown by the solid line. The external potential (24) is shown by the dashed line. The parameters corresponds to the point A in Fig.5: $l = 10$, $d = 1$, $U_0 = 9.8$.

For an estimate the external potential in Fig.7 can be approximated near the top by a parabola, $U \sim -\omega_{\parallel}^2 x^2/2$, with $\omega_{\parallel} \sim 0.5$. This gives the ratio of the typical longitudinal size to the typical transverse size of the contact, $a_{\parallel}/a_t \sim \sqrt{\omega_{\perp}/\omega_{\parallel}} \sim 1$, see also eq. (20). However the selfconsistent potential, Fig.7, is very much different from the simple parabola because of redistribution of electrons along the contact. The selfconsistent potential calculated in the Hartree approximation is practically the same as that calculated in the HF approximation. Nevertheless the HF transmission probability has a shoulder at the point A, see Fig.5, and the Hartree transmission probability has no a shoulder, see Fig.6. The difference is due to the exchange interaction. To demonstrate this we plot in Fig.8 the electron density above the barrier. The HF electron density is shown by the solid line, and the Hartree electron density is shown by the dashed line. We see that the shoulder in the transmission probability is related to the charge density wave above the barrier. There is no a charge density wave in the Hartree approximation, and there is no a shoulder in the corresponding transmission probability shown in Fig.6.

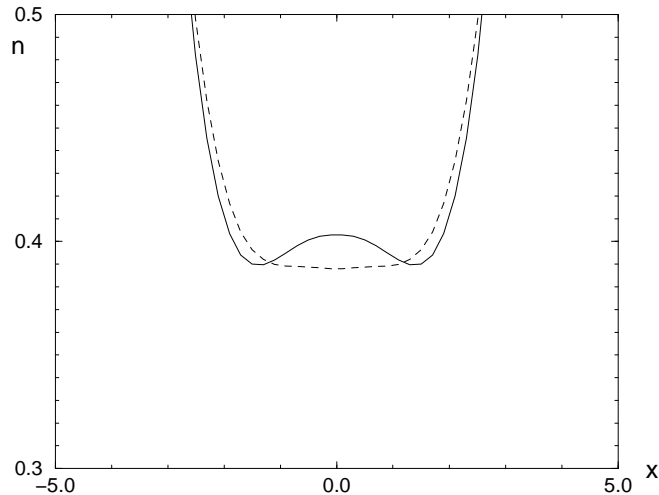


FIG. 8. The electron density on the barrier at $l = 10$, $d = 1$, $U_0 = 9.8$. This corresponds to the shoulder A in Fig.5. The solid line is obtained in the Hartree-Fock approximation and the dashed line is obtained in the Hartree approximation.

The point C in Fig.5 indicates the local minimum at $T \approx 0.5$ for the barrier of the length $l = 16$, the parameters are: $l = 16$, $d = 1$, $U_0 = 11.4$. The corresponding selfconsistent potential is shown in Fig.9 by the solid line, the external potential (24) is shown by the dashed line.

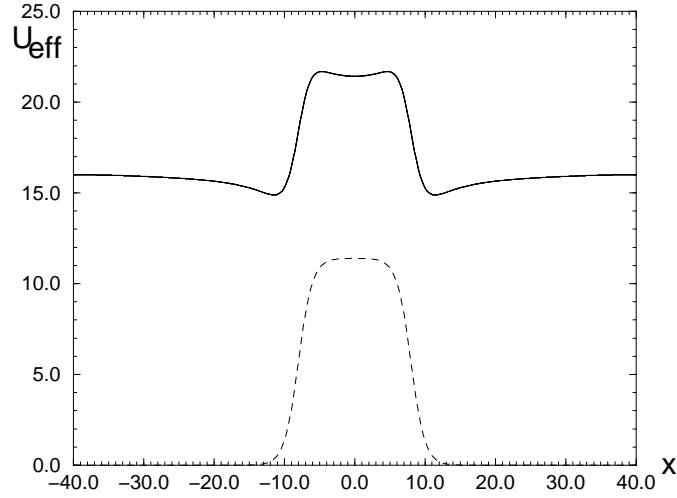


FIG. 9. The selfconsistent HF potential (22) is shown by the solid line. The external potential (24) is shown by the dashed line. The parameters corresponds to the point C in Fig.5: $l = 16$, $d = 1$, $U_0 = 11.4$.

Similar to the previous case the HF selfconsistent potential is practically indistinguishable from the Hartree one. Nevertheless the HF transmission probability has a well pronounced minimum, see point C in Fig.5, and the Hartree transmission probability has just a shoulder, see Fig.6. The difference is due to the exchange interaction. The HF electron density is shown in Fig.10 by the solid line, and the Hartree electron density is shown by the dashed line. There is an additional modulation of the HF density due to the exchange interaction.

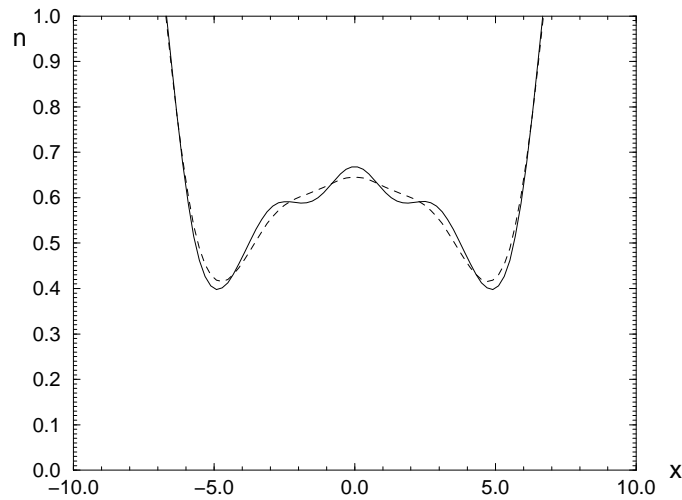


FIG. 10. The electron density on the barrier at $l = 16$, $d = 1$, $U_0 = 11.4$. These parameters correspond to the local minimum C in Fig.5. The solid line corresponds to the Hartree-Fock approximation and the dashed line corresponds to the Hartree approximation.

We see that the structures in the transmission probability are related to the resonance structures above the potential barrier. The resonance structures are related to the charge density waves developing on the barrier when the average electron density above the barrier is of the order of $0.5/a_B$.

V. CONCLUSIONS

The fictitious gauge field method has been developed to calculate a potential barrier transmission probability T with account of many-body effects. The transmission probability is directly related to the conductance, $G = \frac{2e^2}{h}T$. The results of the Hartree-Fock calculations of the transmission probability are shown in Fig.3 and Fig.5. The results demonstrate a plateau or a shoulder at the value of the transmission probability $T \approx 0.7$. For longer barriers this structure is getting weak, but additional structures appear at lower values of T . All the structures are related to the development of the charge density waves on the barrier. This is a precursor for Wigner crystallization. We believe that this explains the conductance anomalies observed in experiments with quantum contacts⁴⁻⁷.

We would like to note that there are two further questions that can be studied within the developed fictitious gauge field approach. The first question is how the structures in the conductance evolve in the external magnetic field. The experimental data⁵ indicates that the conductance anomaly is somehow related to the spin. In the picture considered in the present work the effect is certainly spin dependent because it is due to the exchange interaction. To analyze this problem in details one should perform calculations at $N_\uparrow \neq N_\downarrow$, so the problem is more technically involved compared to the considered case. Another question is the temperature dependence of the anomalies. It is known from experiment that the effect is increasing with temperature up to $\sim 1K$. Unfortunately there is no a direct way to consider the finite temperature case within the developed formalism. However it is clear that any temperature dependence is related to the excitations above the barrier. Moreover there is a direct spectroscopic observation of such excitation⁷. The problem of the collective excitation can be addresses within the developed formalism. To approach this problem one should apply the time dependent Hartree-Fock method in the external gauge field. This calculation is substantially more technically involved compared to the considered case.

I am grateful to P. E. Lindelof who has attracted my attention to this problem. I am also grateful to V. V. Flambaum, C. J. Hamer, M. I. Katsnelson, M. Yu. Kuchiev, A. Nersesyan, D. J. Reilly, and J. Thakur for helpful conversations.

- ¹ D. A. Wharam, T. J. Thornton, R. Newbury, M. Pepper, H. Ritchie, G. A. C. Jones, J. Phys. C **21**, L209 (1988).
² B. J. van Wees, H. van Houten, C. W. J. Beenakker, J. G. Williamson, L. P. Kouwenhoven, D. van der Marel, C. T. Foxton, Phys. Rev. Lett. **60**, 848 (1988).
³ M. Büttiker, Phys. Rev. B **41**, 7906 (1990).
⁴ K. J. Thomas, J. T. Nicholls, M. Y. Simmons, M. Pepper, D. R. Mace, and D. A. Ritchie, Phys. Rev. Lett. **77**, 135 (1996).
⁵ K. J. Thomas, J. T. Nicholls, N. J. Appleyard, M. Y. Simmons, M. Pepper, D. R. Mace, W. R. Tribe, and D. A. Ritchie, Phys. Rev. B **58**, 4846 (1998).
⁶ D. J. Reilly, G. R. Facer, A. S. Dzurak, B. E. Kane, R. G. Clark, P. J. Stiles, A. R. Hamilton, J. L. O'Brien, N. E. Lumpkin, L. N. Pfeiffer, and K. W. West, Phys. Rev. B **63**, 121311 (2001).
⁷ A. Kristensen, H. Bruus, A. E. Hansen, J. B. Jensen, P. E. Lindelof, C. J. Marckmann, J. Nygård, C. B. Sørensen, F. Beuscher, A. Forchel, and M. Michel, Phys. Rev. B **62**, 10950 (2000).
⁸ Chuan-Kui Wang and K.-F. Berggren, Phys. Rev. B **54**, 14257 (1996); Phys. Rev. B **57**, 4552 (1998).
⁹ L. Calmels and A. Gold, Solid State Commun. **106**, 139 (1998).
¹⁰ N. Zabala, M. J. Puska, and R. M. Nieminen, Phys. Rev. Lett. **80**, 3336 (1998).
¹¹ V. V'yurkov and A. Vetrov, cond-mat/0008075.
¹² V. V. Flambaum and M. Yu. Kuchiev, Phys. Rev. B **61**, R7869 (2000).
¹³ T. Rejec, A. Ramsak, and J. H. Jefferson, Phys. Rev. B **62**, 12985 (2000).
¹⁴ E. Lieb and D. Mattis, Phys. Rev. B **125**, 164 (1962).
¹⁵ L. I. Glazman, I. M. Ruzin, and B. I. Shklovskii, Phys. Rev. B **45**, 8454 (1992).
¹⁶ B. Spivak and F. Zhou, Phys. Rev. B **61**, 16730 (2000).
¹⁷ R. Landauer, Z. Phys. **68**, 217 (1987).
¹⁸ For example if $x = 0.1L$ and $y = 0.5L$ then $D = y - x = 0.4L$, however if $x = 0.1L$ and $y = 0.9L$ then $D = 0.2L$.
¹⁹ For the time dependent Hartree-Fock method one shall replace the energy ϵ_i in eq. (21) by the time derivative $-i\partial/\partial t$.
²⁰ V. A. Dzuba, V. V. Flambaum, P. G. Silvestrov, and O. P. Sushkov, Phys. Lett. A **118**, 117 (1986).